Rigidifying Cation-Tunable Nickel Catalysts Increases Activity and Polar Monomer Incorporation in Ethylene and Methyl Acrylate Copolymerization

Babak Tahmouresilerd, Dawei Xiao, and Loi H. Do*

Department of Chemistry, University of Houston, Houston, Texas, 77004

ABSTRACT: In this study, we synthesized and characterized two nickel complexes featuring conformationally rigid bisphosphine mono-oxide ligands, where one has *o*-methoxyphenyl (**Ni2**) and the other has *o*-(2-methoxyethoxy)phenyl (**Ni3**) substituents on the P=O moiety. We performed metal binding studies using **Ni3** and found that its reaction with Li^+ and Na^+ most likely produced 1:1 and 1:1/2:1 nickel-to-alkali species in solution, respectively. The nickel complexes were competent catalysts for ethylene homopolymerization and copolymerization, with activities up to ~3.8×10^3 and 8.1×10^1 kg/mol·h, respectively. In reactions of ethylene with methyl acrylate (1.0 M), the addition of Li^+ to **Ni3** led to greater than 5.4× enhancement in catalyst activity and 1.9× increase in polar monomer incorporation in comparison to that by **Ni3** alone under optimized conditions. A comparison with other nickel catalysts reported for ethylene and methyl acrylate copolymerization revealed that our nickel-alkali catalysts are competitive with some of the most efficient Ni-based systems developed thus far.

INTRODUCTION

Functional polyolefins are an important class of synthetic materials with broad applications in everyday life.[1] Although various methods are available to synthesize functional polyolefins,[2] the coordination-insertion of ethylene and polar olefins is one of the most attractive because it is economical and allows microstructure control of the polymer product.[3-10] To overcome the tendency of nucleophilic monomers to inhibit metal catalysts, which is commonly referred to as the "polar monomer problem," researchers have focused on developing late transition metal catalysts that are less prone to deactivation by Lewis basic donors compared to their early transition metal counterparts.[11] Currently, a diverse array of nickel and palladium complexes have been shown to promote olefin polymerization. Among these, nickel complexes comprising *P*,*O*-donors (e.g., Shell Higher Olefin Process (SHOP)-,[12,13] Drent-,[14] or bisphosphine mono-oxide (BMPO)-type[15,16] complexes; Chart 1A) have stood out due to the lower cost of Ni compared to Pd and their ability to achieve at least moderate polar monomer incorporation (>1 mol% in many cases). The unique reactivity of these Ni(*P*,*O*-donor) complexes has been attributed to their electronic asymmetry,[17] which helps promote olefin insertion into chelated metal intermediates during chain propagation. While these advances are significant, catalysts that can produce copolymers with high molecular weight (e.g., $>10^5$ g/mol) and polar content (e.g., >10 mol%) and at commercially viable rates are still elusive.

Toward the goal of creating the next generation of high-performance olefin polymerization catalysts, we are exploring new strategies to increasing their catalytic rates while simultaneously gaining greater reaction control. Prior to our work, there were early demonstrations that Lewis acid additives could have beneficial effects on olefin polymerization.[18,19] Our laboratory was the first to show that olefin polymerization catalysts could be made cation-tunable by attaching polyethylene glycol (PEG) chains to the ligand framework.[20,21] When paired with select secondary metal ions, these PEGylated complexes formed discrete heterometallic complexes that exhibited distinct reactivity from that of their parent monometallic complexes. In most cases, the cation-promoted catalysts showed improved polymerization activity and gave polymers with higher molecular weight and branching. To assess whether our cation-tuning strategy could be applied to enhance catalysts capable of copolymerizing ethylene and methyl acrylate (MA), we focused our efforts on the palladium phosphine phosphonate ester complex **Pd1** developed by Jordan and coworkers (Chart 1B).[22] To make **Pd1** cation-tunable, we introduced two PEG chains to the phosphonate moiety, which afforded **Pd2**.[23] Our metal binding studies indicated that **Pd2** coordinated with alkali salts to form 1:1 palladium:alkali species (**Pd2**-M, where M = Li^+, Na^+, or K^+). We observed that the **Pd2**-M catalysts displayed higher activity in comparison to that of **Pd2** in ethylene and MA copolymerization but their rates were relatively modest (<9×10^1 kg/mol · h). Because Ni can exhibit greater olefin polymerization activity than Pd in some cases, we next prepared a nickel variant **Ni0** using the same phosphine phosphonate-PEG ligand.[24] Although **Ni0** formed adducts with secondary metals in solution, we have crystallographic characterization of **Ni0**-Na showing that the sodium ion is not bridged by the P=O unit of the ligand. Unfortunately, this dangling sodium did not have significant impact on the catalyst because it is too far away to interact with the nickel center.

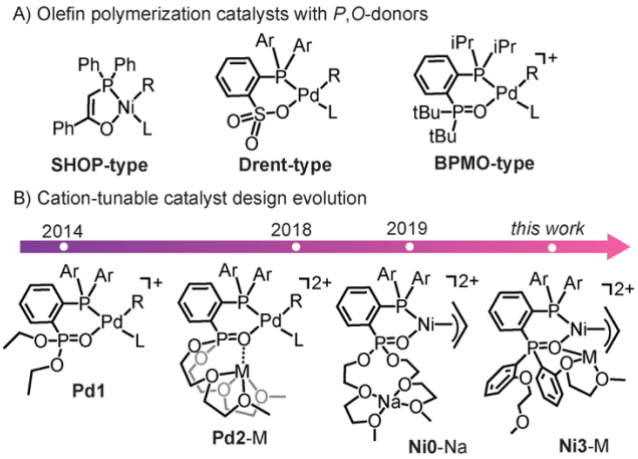

Chart 1. A) Literature examples of nickel olefin polymerization catalysts containing *P*,*O*-donors. B) Design evolution of cation-tunable nickel(*P*,*O*-donor) catalysts developed in the Do laboratory.

To improve our catalyst design, we reasoned that rigidifying the P=O group in **Ni0** by replacing the PEG chains with chelating phenyl substituents would help enforce a short nickel-alkali distance (e.g., **Ni3**-M in Chart 1). By comparing the reactivity of catalysts with varying degrees of conformational flexibility and secondary metal binding affinity, we would be able to gain insights into the structure-function relationships in this family of Ni(*P*,*O*-donor) catalysts. Herein, we report on the results of our rigidified Ni complexes in catalyzing olefin polymerization and discuss how their performance compare to that of other commonly studied Ni catalysts.

RESULTS AND DISCUSSION

Synthesis of Nickel Complexes. The standard catalyst **Ni1** was prepared according to our previously published procedures.[24] To rigidify the P=O side of the nickel complex, we synthesized two new ligand derivatives **6a** (R = methoxy) and **6b** (R = 2-methoxyethoxy) (Scheme 1). Starting from *o*-alkoxybromobenzene, Mg turnings were added to generate the corresponding Grignard reagent, which was then combined with diethyl phosphite to give **2a**/**2b**. Oxidation of this precursor using H_2O_2 under basic conditions afforded **3a**/**3b** as a white solid. This compound was then combined with thionyl chloride to provide the phosphinic chloride **4a**/**4b**. To assemble the full ligand, compound **5** was treated with *n*-butyllithium and then reacted with **4a**/**4b** to furnish the desired *P*,*O*-ligands**.** Although this last step was low yielding (≤ 45%), the previous steps were relatively efficient (> 60% yield). Finally, to obtain the nickel complexes **Ni2** and **Ni3**, their corresponding *P*,*O*-ligands were stirred in the presence of [Ni(allyl)Cl]$_2$ and $AgSbF_6$ for several hours and the desired complexes were isolated as yellow solids in 85 and 75% yield, respectively. The

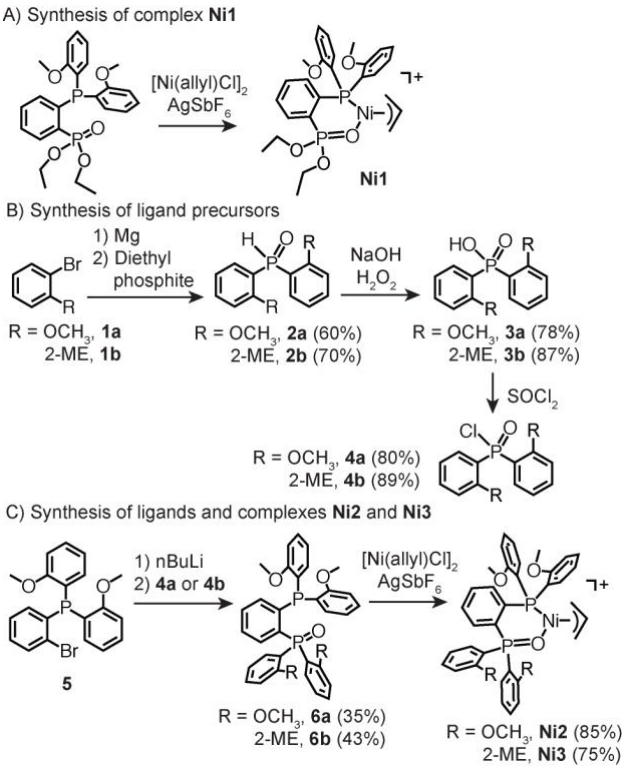

Scheme 1. Synthetic procedures for the preparation of **Ni1**, **Ni2**, and **Ni3**. 2-ME = 2-methoxyethoxy ($OCH_2CH_2OCH_3$).

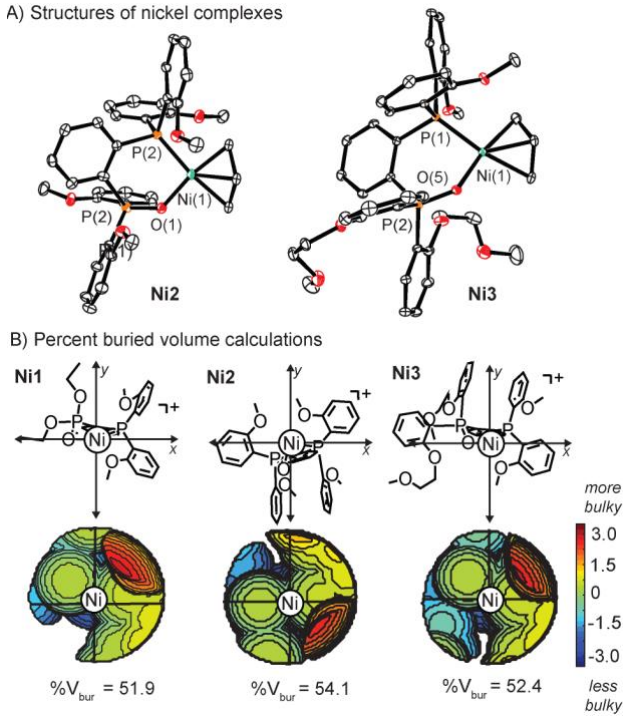

Figure 1. A) Molecular structures of **Ni2** and **Ni3** characterized by single crystal X-ray crystallography. The structures are shown in ORTEP view with displacement ellipsoids drawn at 50% probability. Hydrogen atoms and the SbF_6^- have been omitted for clarity. B) Topographical steric maps of **Ni1**, **Ni2**, and **Ni3** derived from their crystallographic data using SambVca 2.1. Only the *P*,*O*-ligands were considered in the calculation of $\%V_{bur}$. The nickel atom was set as the center of the coordination sphere, the nickel square plane defined the *xz*-plane, and the *z*-axis bisects the P–Ni–O angle.

nickel complexes were fully characterized by NMR spectroscopy and elemental analysis.

Characterization of Nickel Complexes. Single crystals of **Ni2** and **Ni3** were grown by slow diffusion of pentane into a solution of the complexes in CH_2Cl_2. Analysis by X-ray diffraction revealed that both nickel centers are ligated by a *P*,*O*-donor and an allyl anion, giving the molecular formulas [Ni(**6a**)(η^3-allyl)]SbF_6 for **Ni2** and [Ni(**6b**)(η^3-allyl)]SbF_6 for **Ni3** (Figure 1A). Both **Ni2** and **Ni3** adopt pseudo square planar geometries, similar to that in **Ni1**. To determine the steric effects of having different ancillary groups, we compared the structural parameters between **Ni1**,[24] **Ni2**, and **Ni3** (Table 1). Although their Ni-P, Ni-O, and Ni-C′ bond distances varied slightly from one another (average = ~2.19, 1.90, and 1.98 Å, respectively), they differed at most up to ~0.03 Å. However, the three nickel complexes displayed clear differences in their geometric distortions. For example, the P′-O-Ni-P torsion angles of 6.69, 12.88, and 38.91° for **Ni1**, **Ni2**, and **Ni3**, respectively, indicate increasing deviation from a planar nickel chelate as defined by the *P*,*O*-ligand. Their C-P-Ni-O torsion angles are also noticeably different, at 34.96, 27.02, and 47.66° for **Ni1**, **Ni2**, and **Ni3**, respectively.

Using the crystallographic data above, we calculated the percent buried volume ($\%V_{bur}$) of the nickel complexes, which provide a quantitative measure of the steric bulk of the *P*,*O*-donor within a 3.5 Å radius around the nickel coordination sphere. Our results showed that the $\%V_{bur}$ of the nickel

Table 1. Comparison of Structural Parameters[a]

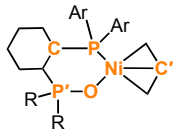

Metric	Ni1	Ni2	Ni3
Ni–P (Å)	2.198	2.204	2.184
Ni–O (Å)	1.915	1.881	1.906
Ni–C′ (Å)	2.002	1.984	1.969
O–Ni–P (Å)	97.27	97.63	91.13
C–P–Ni–O (°)	34.96	27.02	47.66
P′–O–Ni–P (°)	6.69	12.88	38.91

[a]Crystallographic data for **Ni1** were reported previously. A simplified depiction of the nickel center is shown above using orange letters to indicate the atoms of interest.

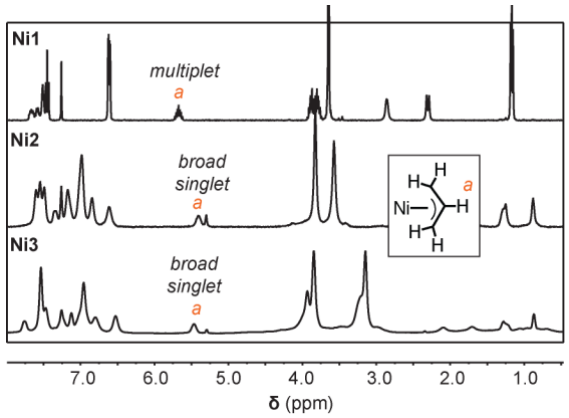

Figure 2. Stacked ^{1}H NMR spectra ($CDCl_3$, 500 MHz) of the nickel complexes at RT.

complexes are quite similar, with values of 51.9, 54.1, and 52.4% for **Ni1**, **Ni2**, and **Ni3**, respectively (Figure 1B). However, because we were unable to obtain crystallographic characterization of the corresponding nickel-alkali complexes (*vide infra*), it is unclear how secondary metal binding to the nickel complexes impacts their steric profiles.

To study the solution structure of the nickel complexes, we recorded their ^{1}H NMR spectra in $CDCl_3$ at RT. As shown in Figure 2, **Ni1** displayed sharp NMR peaks between 1-8 ppm. The central allyl hydrogen atom (H_a) appeared as a multiplet at 5.67 ppm. Surprisingly, both **Ni2** and **Ni3** gave NMR spectra with broad signals. For example, although the H_a peaks for **Ni2** and **Ni3** were observed at ~5.4 ppm, they appeared as single broad resonances. Increasing the solution temperature up to 80 °C did not lead to peak sharpening. These NMR data suggest that while bond rotation in **Ni1** is fast on the NMR timescale, it is significantly slower in **Ni2** and **Ni3**. We hypothesize that this difference is due to rigidification of the nickel structure by the presence of the P=O phenyl groups in the latter complexes. We will show in our polymerization studies below that these structural features strongly influence their catalytic behavior.

Next, the electrochemical properties of the nickel complexes were measured using cyclic voltammetry (Figure S42). We observed that in THF, **Ni1**, **Ni2**, and **Ni3** showed irreversible reduction waves at -2.28, -2.49, and -2.54 V (vs. ferrocene/ferrocenium), respectively. As control, the *P,O*-ligands themselves were found to be redox inactive. The reduction peaks in the nickel complexes were tentatively assigned to metal-centered reduction of Ni(II) to Ni(I).[25-27]

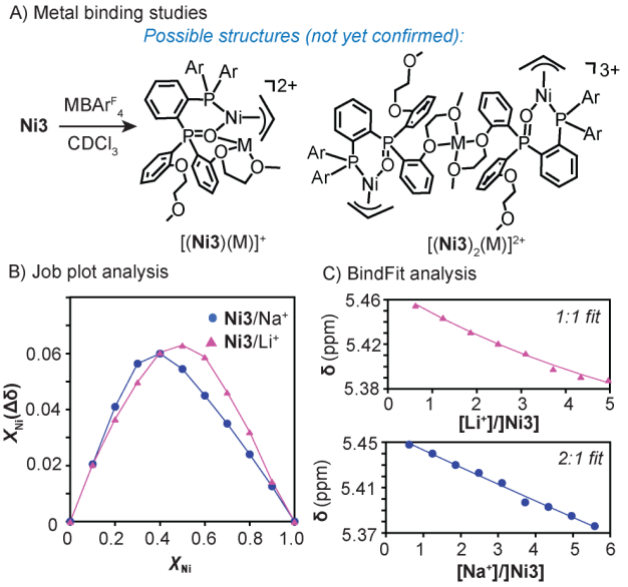

Figure 3. A) Reaction of $MBAr^F_3$ (M = Li^+ or Na^+) with **Ni3**. Possible structures for the 1:1 and 2:1 nickel: alkali species are shown but have not yet been confirmed. B) Job plot analysis of metal binding studies using **Ni3**/Li^+ and **Ni3**/Na^+ gave peak maxima at X_{Ni} = 0.5 and 0.4, respectively. C) Bindfit global analysis of metal titration data yielded satisfactory fits using a 1:1 model for **Ni3**/Li^+ and 2:1 model for **Ni3**/Na^+, respectively.

These results suggest that **Ni1** is the most electron deficient in the series and **Ni2** and **Ni3** are similar electronically.

Metal Binding Studies. In previous work, we demonstrated that **Ni1** interacts weakly with secondary metals, most likely via coordination by the P=O moiety.[24] Because **Ni3** is predicted to have greater affinity for external cations than **Ni2** (i.e., 2-methoxyethoxy is a stronger metal chelator than methoxy), we focused our metal binding studies on the former. To conduct these experiments, we prepared $CDCl_3$ solutions containing mixtures of **Ni3** and $MBAr^F_4$ (where M = Na^+ or Li^+, $BAr^F_4{}^-$ = tetrakis(3,5-trifluoromethylphenyl)borate) in different ratios with a total concentration of 6 mM. When the samples were measured by ^{1}H NMR spectroscopy, we observed that the presence of increasing amounts of alkali ions relative to nickel led to an upfield shift of the H_a resonance in **Ni3** (Figures S1-S2). A Job Pot of the NMR data revealed a peak maximum at X_{Ni} = 0.5 and 0.4 for **Ni3**/Li^+ and **Ni3**/Na^+, respectively (where X_{Ni} = [**Ni3**]/([**Ni3**]+[M^+]). These results suggest that the optimal nickel:alkali stoichiometry is 1:1 for **Ni3**/Li^+ but not for **Ni3**/Na^+.[28] A possible limitation of these metal binding studies is that they must be performed in chloroform, not the polymerization solvent dichloromethane/toluene (2:48), due to the low solubility of the alkali salts in non-coordinating solvents.

To investigate further the host-guest interactions of **Ni3** with alkali ions, we carried out metal titration studies using ^{1}H NMR spectroscopy. As expected, addition of up to ~5 equiv. of $MBAr^F_4$ to a $CDCl_3$ solution containing **Ni3** (20 μM) resulted in an upfield shift of the H_a signal. The titration data were subjected to global fit analysis using the program BindFit.[29-31] Three different binding models were evaluated, including 1:1 (Eq. 1), 2:1 (Eqs. 1 and 2), and 1:2 (Eqs. 1 and 3) nickel and alkali reactions.

Table 2. Ethylene Hompolymerization Studies[a]

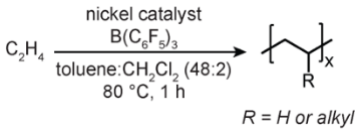

Entry	Catalyst (μmol)	Salt	C_2H_4 (psi)	Polymer Yield (g)	Activity (kg/mol·h)	Branches (/1000 C)[b]	M_n ($\times 10^3$)[c]	$Đ$[c]	Polymers/ Catalyst
1	**Ni1** (1.0)	none	200	0.643	643	4	0.5	2.6	129
2	**Ni1** (1.0)	Li^+	200	0.744	744	7	1.6	1.3	47
3[d]	**Ni2** (5.0)	none	200	19.2	3840	15	10.2	1.6	188
4[d]	**Ni2** (5.0)	Na^+	200	27.2	5440	14	12.6	1.5	216
5[d]	**Ni2** (2.0)	None	200	5.17	2588	4	19.3	1.2	27
6	**Ni2** (1.0)	None	200	0.753	753	4	47.0	1.2	2
7	**Ni2** (0.5)	None	200	0.217	434	4	26.1	1.2	1
8	**Ni2** (1.0)	Li^+	200	0.768	768	4	22.3	1.2	3
9	**Ni2** (1.0)	Na^+	200	0.885	885	4	21.7	1.2	4
10	**Ni2** (1.0)	None	300	1.12	1120	5	26.9	1.2	4
11	**Ni2** (1.0)	Na^+	300	1.16	1160	4	27.6	1.2	4
12	**Ni2** (1.0)	None	400	1.21	1210	2	28.1	1.2	4
13	**Ni3** (1.0)	None	200	3.81	3810	5	6.6	1.2	58
14	**Ni3** (1.0)	Li^+	200	8.81	8810	5	8.4	1.2	105
15	**Ni3** (1.0)	Na^+	200	8.43	8430	7	8.1	1.2	104
16	**Ni3** (1.0)	K^+	200	5.48	5480	7	7.4	1.2	74
17	**Ni3** (1.0)	Cs^+	200	4.96	4960	7	7.9	1.2	63

[a]Polymerization conditions: Ni catalyst (varied), ethylene (varied), $B(C_6F_5)_3$ (2.0 equiv.), $MBAr^F_4$ (1.1 equiv., if any), 2 mL of DCM, 48 mL of toluene, 1 h at 80 °C. The activity provided is the average of at least duplicate runs. [b]The total number of branches per 1000 carbons was determined by ^{1}H NMR spectroscopy. [c]The M_n and $Đ$ values were determined by GPC in 1,2,4-trichlorobenzene at 160 °C. [d]The reaction was highly exothermic, causing the solution temperature to increase above 80 °C.

The equilibrium expressions are given below:

$$[\mathbf{Ni3}]^+ + M^+ \rightleftharpoons [(\mathbf{Ni3})(M)]^{2+} \qquad (1)$$

$$[(\mathbf{Ni3})(M)]^{2+} + [\mathbf{Ni3}]^+ \rightleftharpoons [(\mathbf{Ni3})_2(M)]^{3+} \qquad (2)$$

$$[(\mathbf{Ni3})(M)]^{2+} + M^+ \rightleftharpoons [(\mathbf{Ni3})(M)_2]^{3+} \qquad (3)$$

For both **Ni3**/Li^+ (Figure S5) and **Ni3**/Na^+ (Figure S6), the 1:1 and 2:1 models gave satisfactory fits. The 1:2 models were ruled out due to the >100% error associated with the binding constants derived from the fits.

Taking into consideration results from both the Job Plot and BindFit analyses, we propose that the reaction of **Ni3** with Li^+ most likely produced $[(\mathbf{Ni3})(Li)]^{2+}$ with a binding constant of 3.6 M^{-1} (Figure 3C, top). In contrast, the reaction of **Ni3** with Na^+ most likely produced both $[(\mathbf{Ni3})(Na)]^{2+}$ and $[(\mathbf{Ni3})_2(Na)]^{3+}$ species in solution, with binding constants of 51.7 and 996.0 M^{-1} (Figure 3C, bottom). Although attempts to grow single crystals of the purported $[(\mathbf{Ni3})(M)]^{2+}$ and $[(\mathbf{Ni3})_2(M)]^{3+}$ species for X-ray crystallographic analysis have not yet been successful, some possible structures are shown in Figure 3A. For the $[(\mathbf{Ni3})(M)]^{2+}$ species, we favor binding of M^+ by only one 2-methoxyethoxy arm because chelation by both may be too strained. For the $[(\mathbf{Ni3})_2(M)]^{3+}$ species, we propose a structure in which two nickel complexes are bridged by a single M^+ ion. A similar trinuclear species was reported by our group for the nickel phenoxyimine-PEG complexes.[20] Regardless of their molecular structures, our polymerization results below indicate that the nickel-alkali species display distinct reactivity in comparison to that of their parent mononickel complexes.

Ethylene Homopolymerization. To test the catalytic activity of the nickel complexes, we evaluated their ability to polymerize ethylene under various reaction conditions. All reactions were performed in 50 mL of CH_2Cl_2/toluene (2:48) by combining the nickel complex with 2 equiv. of the $B(C_6F_5)_3$ activator under 200 psi of ethylene at 80 ° C. Although the nickel complexes can self-initiate in the absence of a cocatalyst at 100 °C with high Ni loading (Table S7, entry 2 vs. 3), we found that the addition of boranes significantly improved their polymerization efficiency. This strategy has also been used successfully by others to activate structurally similar nickel η^3-allyl species for olefin polymerization.[32,33] We hypothesize that the borane promotes conversion of the coordinated allyl ligand from η^3 to η^1, which favors subsequent olefin binding and insertion. Our NMR studies indicate that catalyst activation using $B(C_6F_5)_3$ occurs only at elevated temperatures. For example, at room temperature, combining **Ni3** with $B(C_6F_5)_3$ led to only slight broadening of the ^{1}H NMR spectra of the nickel complex and nearly no change in the ^{11}B resonance of the borane (Figure S58). These results suggest that $B(C_6F_5)_3$ does not interact strongly with the **Ni3** PEG chain, if at all. When the solution temperature was increased to 50 °C, the ^{1}H NMR spectrum showed numerous new peaks, which we were unable to assign. In the absence of olefin monomers, the activated nickel species is not likely to be chemically stable.

Table 3. Ethylene and Methyl Acrylate Copolymerization Studies[a]

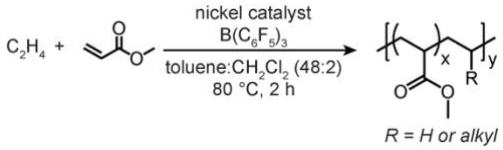

Entry	Catalyst	Salt (equiv.)	MA (M)	Copolymer Yield (mg)	Activity (kg/mol· h)	M_n ($\times 10^3$)[b]	$Đ$[b]	Inc. (mol%)[c]	MA per Chain[d]	MA In-Chain (%)
1	**Ni1**	none	0.1	312	15.6	0.6	6.5	0.29	0.06	64
2	**Ni2**	none	0.1	438	21.9	6.3	2.1	0.30	0.67	90
3	**Ni3**	none	0.1	566	28.3	5.2	1.8	0.36	0.66	86
4	**Ni1**	Li (1.1)	0.1	490	24.0	1.1	1.5	0.32	0.12	68
5	**Ni2**	Li (1.1)	0.1	725	36.0	9.4	1.6	0.39	1.30	88
6	**Ni3**	Li (1.1)	0.1	1630	81.0	6.2	1.9	0.52	1.14	72
7	-	Li (1.1)	0.5	0	0	-	-	-	-	-
8	**Ni3**	none	0.5	219	10.9	4.2	1.4	1.00	1.47	91
9[e]	**Ni3**	none	0.5	360	18.0	2.9	1.4	1.30	1.31	91
10[f]	**Ni3**	none	0.5	30	1.5	2.8	2.1	0.96	0.94	-
11	**Ni3**	Li (1.1)	0.5	408	20.3	3.1	1.7	1.30	1.40	88
12	**Ni3**	Li (5.0)	0.5	147	7.3	3.7	1.9	1.30	1.67	-
13	**Ni3**	none	1.0	36	1.8	2.2	1.4	2.40	1.80	99
14	**Ni3**	Li (1.1)	1.0	196	9.8	2.5	1.5	4.50	3.68	99
15	**Ni3**	Na (1.1)	1.0	142	7.1	2.9	1.1	8.10	7.18	-

[a]Polymerization conditions: Ni catalyst (10 μmol), ethylene (400 psi), $B(C_6F_5)_3$ (2.0 equiv.), $MBAr^F{}_4$ (1.1 equiv., if any), 2 mL of DCM, 48 mL of toluene, 2 h at 80 °C. The activity provided is the average of at least duplicate runs. [b]The M_n and $Đ$ values were determined by GPC in 1,2,4-trichlorobenzene at 160 °C. [c]The methyl acrylate incorporation was determined using ^{1}H NMR spectroscopy. [d]See the supporting information for the MA per chain calculation. [e]A total of 10.0 equiv. of $B(C_6F_5)_3$ was used. [f]No $B(C_6F_5)_3$ was used.

In our polymerization studies, we found that when 5.0 μmol of **Ni2** was used, the reaction was highly exothermic and caused the reaction mixture to increase in temperature from 80 to 120 ° C (Table 2, entry 3).The semicrystalline polyethylene (PE) obtained was characterized and determined to have low branching (~15/1000 carbons) and low molecular weight (M_n = 10.2 kg/mol), which is typical for this family of catalysts.[22] The presence of alkenyl peaks in the polymer NMR spectra indicate that polymerization terminates via chain transfer.[5] To minimize temperature fluctuations during polymerizations, different catalyst amounts were screened from 0.5 to 2.0 μmol (entries 5-7). Because reactions using 1.0 μmol of **Ni2** did not increase the reactor temperature and gave the most consistent results, all subsequent studies were performed using this catalyst loading. Varying the ethylene pressure from 200 to 400 psi led to almost proportional increase in catalyst activity (entries 6, 10, and 12), suggesting that the reaction may be first order in monomer. Under optimized conditions (Table 2), the nickel catalysts showed the activity trend **Ni1** (entry 1) < **Ni2** (entry 6) < **N3** (entry 13). Catalyst **Ni2** (7.5×10^2 kg/mol·h) and **Ni3** (3.8×10^3 kg/mol·h) were about 1.2× and 5.9× more active than **Ni1** (6.4×10^2 kg/mol·h), respectively. Interestingly, the PE obtained from **Ni2** (47.0 kg/mol) and **Ni3** (6.6 kg/mol) were also higher in molecular weight than that obtained from **Ni1** (0.5 kg/mol). The PEs produced were all highly linear (≤ 15 branches/ 1000 carbons). Given that the three nickel complexes have similar steric encumbrance, these results suggest that differences in their reactivity may be attributed at least in part to differences in their conformational flexibility. Perhaps the more rigid complexes **Ni2** and **Ni3** can better maintain their structural integrity during catalysis and are less prone to catalyst deactivation than **Ni1**. In fact, time studies showed that **Ni1** has highest polymerization activity at 0.5 h and decreased by ~0.66× after 1.5 h (Table S6). In contrast, **Ni3** exhibited highest activity at 1.0 h and decreased by only ~0.27× after 1.5 h. The observation that **Ni3** (entry 6) was significantly more active than **Ni2** (entry 13) suggests that steric bulk (%V_{bur} = 54.1 and 52.4, respectively) is not strongly correlated with catalyst activity. The benefits of having rigid catalyst structures on polymerization performance has been documented in other studies, such as those showing that catalysts with five- and six-membered chelate rings were significantly more active than those with seven-membered ones.[34,35] Presumably, catalysts with greater structural flexibility are susceptible to side reactions or decomposition.

Next, we explored whether our nickel complexes could be tuned using external cations. For these experiments, the catalysts were screened under our standard ethylene polymerization conditions with the addition of 1.1 equiv. of $MBAr^F{}_4$ (Table 2). In all cases, we observed that reactions containing alkali salts produced higher yields of PE in comparison to those without additives. For example, the addition of Li^+ to **Ni1** (entry 2), **Ni2** (entry 8), and **Ni3** (entry 14) led to a 1.16 ×, 1.02 ×, and 2.31 × enhancement in polymerization rates, respectively. The activity increase for **Ni1** and **Ni2** is modest most likely because their interactions with the alkali ions are weak, which may lead to dissociation of the coordinated M^+ ion during polymerization. In contrast, the **Ni3** catalyst that was designed to bind secondary metals with higher affinity, has a more significant response to M^+. Interestingly, although the introduction of Li^+, Na^+, K^+, and Cs^+ to **Ni3** led to varying degrees of activity enhancement (entries 14-17), the PEs generated have similar molecular weights (M_n = 6.6-8.4 kg/mol). These results suggest that the alkali ions increase the

rates of chain growth (v_{growth}) and chain transfer ($v_{transfer}$) by approximately the same magnitude ($v_{growth}/v_{transfer}$ = ~300).[36] Although nearly all catalyst gave polymers with narrow molecular weight distributions ($Đ$ <2), they are non-living as indicated by their ability to produce multiple polymers per metal.

Because our mononickel complexes are cationic with SbF_6^- counterions, we next investigated whether the addition of salts with different anions have any effects on polymerization. We found that ethylene polymerizations using [**Ni3**]SbF_6 with $NaBArF_4$, $NaB(C_6F_5)_3$, or $NaSbF_6$ salts under the same reaction conditions gave yields of 1.44, 1,42, and 1.28 g (Table S8), respectively, which suggest that there is a slight but not dramatic effect of mixing non-coordinating anions on polymerization.

The cation boosting effects observed in this work appear to be a general phenomenon since it also occurs using other olefin polymerization catalysts.[18,37] We showed in previous studies that cation binding can increase a catalyst's steric bulk as well as electrophilicity.[38] Due to differences in their chemical nature, secondary metals can alter a catalyst's structural and electronic characteristics to different extents, which makes this tuning strategy extremely powerful. Our ethylene homopolymerization results for **Ni1**, **Ni2**, and **Ni3** (Table 2) clearly showed that increasing catalyst rigidity and introducing secondary metals

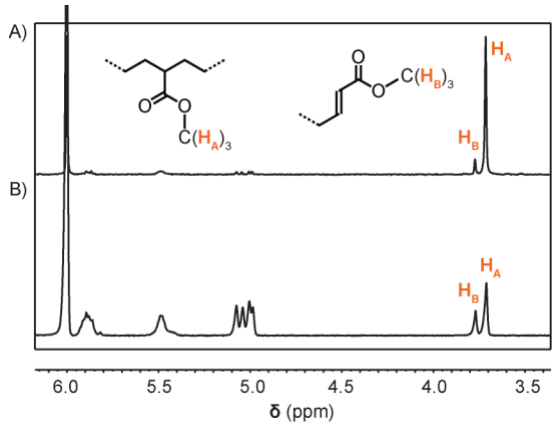

Figure 4. Representation examples of the ^{1}H NMR spectra ($C_2D_2Cl_4$, 500 MHz, 120 °C) obtained for ethylene/MA copolymers in this study. The polymerization conditions are given in Table 3, entries 8 (A, top) and 4 (B, bottom).

are effective strategies to enhance the polymerization performance of this family of Ni(*P*,*O*-donor) catalysts.

Ethylene and Methyl Acrylate Copolymerization. After establishing their baseline reactivity with ethylene, the nickel catalysts were next tested for their ability to copolymerize ethylene with methyl acrylate (MA). Initially, we combined the nickel complex, $B(C_6F_5)_3$, and MA in a reaction vial prior to injecting the mixture into an autoclave and pressurizing with ethylene. However, we observed that this procedure produced significant amounts of poly(methyl acrylate) (PMA). When the reaction was carried out without ethylene, only trace amounts of PMA were obtained. It should be noted that the amount of excess $B(C_6F_5)_3$ (10 μmol) used in copolymerization is far lower than that of MA present (≥ 5000 μmol) so any borane interactions with the monomer are minimal. To avoid generating PMA, we modified our protocol so that the nickel complex and $B(C_6F_5)_3$ were first dissolved in CH_2Cl_2/toluene and then the mixture was injected into a CH_2Cl_2/toluene solution containing methyl acrylate and ethylene (pre-saturated). The autoclave pressure was increased to 400 psi of ethylene and the reaction was stirred at 80 ℃ for 2 h. In the presence of 0.1 M methyl acrylate (Table 3), all three nickel catalysts furnished semicrystalline polymers with activities of 1.56×10^1 (entry 1), 2.19×10^1 (entry 2), and 2.83×10^1 kg/mol·h (entry 3) for **Ni1**, **Ni2**, and **Ni3**, respectively. The polymer products were washed with acetone/methanol and no PMA was found in any of the washings. Characterization of the purified materials by NMR spectroscopy revealed distinct peaks corresponding to incorporated MA units,[14,22] suggesting that the product is the desired ethylene/MA copolymer. Their NMR spectra indicated that their MA units are predominantly in-chain (64-99%, Figure 4), which means that ethylene can insert into the nickelacycle generated from a previous MA insertion step (i.e., MA insertion does not necessarily lead to chain termination). In terms of MA incorporation efficiency, the catalysts showed the trend **Ni1**< **Ni2** < **Ni3**, with MA incorporations of 0.29, 0.30, and 0.36 mol%, respectively. However, taking into account the polymer MW and MA incorporation percentage, all three polymers were calculated to have on average <1.0 MA per chain.

Interestingly, adding 1.1 equiv. of Li^+ to the nickel catalysts led to noticeable improvements in copolymerization efficiency. For example, combining **Ni3**/$LiBArF_4$ with ethylene and MA gave catalyst activity of 8.10×10^1 kg/mol·h (Table 3, entry 6), which is 2.9× higher than that observed for reactions lacking Li^+ (entry 3). We found that the copolymers obtained from **Ni1**/Li^+ (entry 4), **Ni2**/Li^+ (entry 5), and **Ni3**/Li^+ (entry 6) contained about 1.1×, 1.3×, and 1.4× greater amounts of MA, respectively, than those produced from their parent mononickel catalysts. When the concentration of MA was increased, the catalyst activity decreased but the MA incorporation percentage was generally higher. Using 1.0 M concentration of MA (entry 14), **Ni3**/Li^+ afforded copolymers with 4.5 mol% of the polar olefin, which is approximately 3.7 MA units per chain. Although **Ni3**/Na^+ produced copolymers with slightly higher MA content (8.1 mol%, entry 15) than **Ni3**/Li^+, its activity was lower so no further studies were pursued using Na^+. The greater increase in catalyst activity using Li^+ compared to Na^+ has been attributed to the greater Lewis acidity of the former relative to the latter.[38]

As a control, reactions using just $LiBArF_4$ and $B(C_6F_5)_3$ without Ni catalyst and in the presence of ethylene/MA did not generate any polymers (Table 3, entry 7). These results suggest that the copolymers obtained were likely formed via coordination-insertion[5] rather than cationic polymerization mechanisms.[39] Finally, adding 5.0 equiv. of $LiBArF_4$ to the nickel catalyst led to a drop in activity (e.g., entry 11 vs. 12). Since the optimal **Ni3** to Li^+ stoichiometry was determined to be 1:1, perhaps the presence of excess Li^+ causes formation of other multinuclear species that are not catalytically active. It is noteworthy that in all polymerization reactions using **Ni1**, **Ni2**, or **Ni3** with $MBArF_4$, the polymer dispersity values are narrow ($Đ \leq 2.0$), which is indicative of single site catalysis.

Comparison with Other Ni Catalysts. To assess the overall performance of different nickel catalysts reported in the literature, it is useful to compare three key metrics: catalyst activity, polymer molecular weight, and MA per chain. We analyzed the ethylene and MA copolymerization data from recent studies and selected the most promising examples from each work (Table S9). Because it is useful to compare catalysts

under their optimal conditions, some of these reactions may differ in temperature, pressure, or monomer concentration. To visualize the data, we created a color-coded plot showing log(MA per chain) vs. log(M_n) observed for the different complexes (Figure 5). The color of each dot (red, yellow, or green) indicates the relative activity of that catalyst. The nickel complexes chosen are supported by different bidentate ligands,

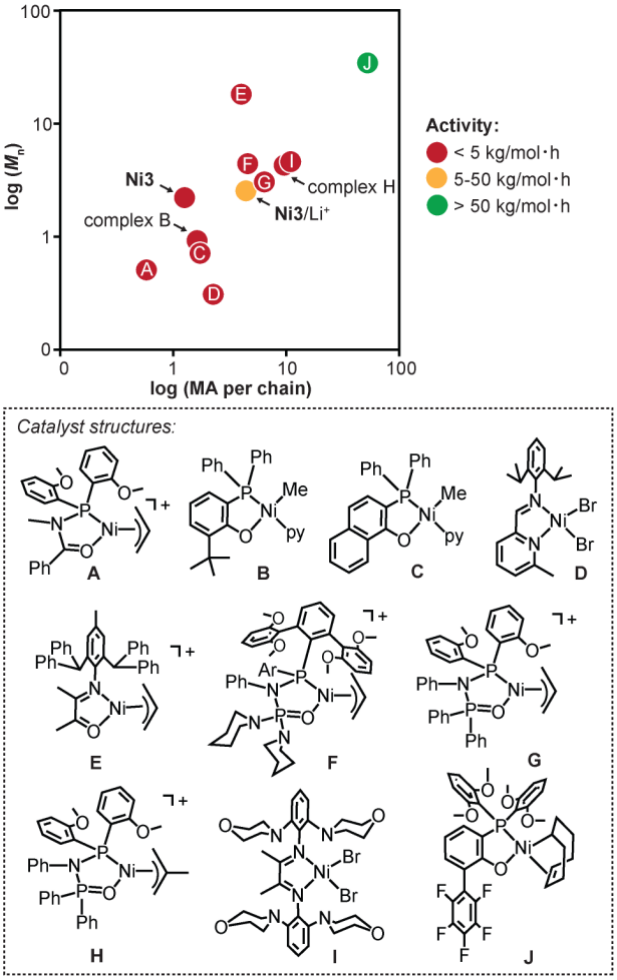

Figure 5. Comparison of various nickel catalysts reported in the literature for ethylene and methyl acrylate copolymerization. The plot shows the polymer M_n, MA per chain, and activity of the different catalysts. The data for complexes **A**, **B**, **C**, **D**, **E**, **F**, **G**, **H**, and **I** are given in Table S9. These examples were selected because they represented some of the highest MA incorporations achieved in the different studies.

including keto-phosphine (**A**[40]), aryloxyphosphine (**B**,[41] **C**,[42] **J**[43]), imino-pyridine (**D**[44]), keto-imine (**E**[45]), bisphosphine mono-oxide (**F**,[46] **G**,[47] **H**[48]), and diimine (**I**[49]) donors. The plot in Figure 5 revealed several interesting trends. First, it appears that some catalysts exhibit markedly different behaviors than that of their structurally similar variants while others are similar. For example, within the Ni aryloxyphosphine family, complex **B** gave copolymers with low molecular weight (0.9 kg/mol) and low MA per chain (0.55) whereas complex **J** gave copolymers with moderate molecular weight (34 kg/mol) and high MA per chain (~50). In contrast, catalysts **F**, **G**, and **H** in the Ni bisphosphine mono-oxide family all produced copolymers with similar characteristics (M_n = 3.0-4.3 kg/mol, MA per chain = 4-9). Second, although the Ni catalysts all successfully catalyzed ethylene and MA copolymerization, they typically showed low activity (<5 kg/mol·h) with the exception of **J** (86 kg/ kg/mol·h). The reduced reactivity of metal catalysts in the presence of functional olefins is attributed to σ-coordination of the polar group to the active catalyst or back-chelation by an inserted polar monomer.[50] Third, the symmetric catalyst **I** appears to perform just as well, if not better, than most of the asymmetric catalysts. Thus, it is unclear if asymmetric catalysts have any intrinsic advantages over symmetric ones in terms of their ability to copolymerize polar monomers.[17] While these literature examples indicate that further development is needed to obtain commercially viable catalysts, some breakthrough examples such as complex **J** suggest that the "polar monomer problem" can be overcome. In fact, a recent report of a dinickel SHOP-type catalyst for ethylene and *tert*-butyl acrylate copolymerization (activity = 82 kg/ kg/mol·h; M_n = 9 kg/mol; *tert*-butyl acrylate per chain = 29)[51] lends credence to this optimistic outlook.

In comparison to other nickel catalysts reported in the literature, mononuclear **Ni3** showed reactivity in line with many other Ni(*P*,*O*-donor) complexes (Figure 5). Interestingly, the addition of Li^+ to **Ni3** led to clear improvements in reaction efficiency and MA per chain without diminishing polymer molecular weight. The activity of **Ni3**/Li^+ in ethylene and MA copolymerization exceeded the 5 kg/mol·h limit typical of most Ni catalysts. The performance of **Ni3**/Li^+ is similar to that of our first-generation palladium-PEG catalyst with Li^+ (**Pd2**-Li, Chart 1).[23] However, because palladium is a precious metal whereas nickel is not, these results are promising from a sustainability standpoint.

CONCLUSION

In summary, to study the effects of ligand rigidification on our nickel(*P*,*O*-donor) complexes, we developed two new variants **Ni2** and **Ni3** containing *o*-methoxyphenyl and *o*-(2-methoxyethoxy)phenyl substituents, respectively. For comparison, the parent complex **Ni1** featuring ethoxy groups attached to the P=O moiety were also synthesized. Using the crystallographic data from the Ni complexes, we calculated the %V_{bur} of their *P*,*O*-donors and determined that all three ligands in **Ni1**-**Ni3** have similar steric volumes (~51-54%). However, we found that both **Ni2** and **Ni3** gave NMR spectra with broad peaks in $CDCl_3$, suggesting that the complexes are conformationally restricted in solution. In contrast, the NMR peaks corresponding to **Ni1** are sharp, which indicates that the complex has fast bond rotation on the NMR timescale. On the basis of our metal binding studies, we propose that **Ni3** forms 1:1 adducts with Li^+ ($[(\mathbf{Ni3})(Li)]^{2+}$), whereas it forms 1:1 ($[(\mathbf{Ni3})(Na)]^{2+}$) and 2:1 ($[(\mathbf{Ni3})_2(Na)]^{3+}$) adducts with Na^+. In ethylene homopolymerization studies, we showed that **Ni2** and **Ni3** were both more active and produced polymers with higher molecular weight than **Ni1**. Presumably, the greater structural rigidity in the former enhanced their catalyst lifetimes relative to that of the latter. Consistent with our previous results, introducing alkali ions to the nickel complexes increased their catalyst efficiency and MA incorporation. Complex **Ni3**, which features the strongest secondary metal chelator within the nickel series, gave the most dramatic response to M^+. Relative to other Ni catalysts reported for ethylene and MA copolymerization, **Ni3**/Li^+ performed average in terms of polymer MW and MA per chain but above average in catalyst activity. Given that there are still many ways to optimize our nickel complexes, including

by covalent ligand modifications and cation-tuning, we are optimistic that future breakthroughs in Ni(*O*,*P*-donor) catalyst designs are possible.

ASSOCIATED CONTENT

Supporting Information

The Supporting Information is available free of charge on the ACS Publications website.

Experimental procedures, spectroscopic data, and metal binding studies (PDF)

Crystallographic data (CIF)

AUTHOR INFORMATION

Corresponding Author

Loi H. Do - Department of Chemistry, University of Houston, 4800 Calhoun Rd., Houston, Texas 77204, United States; Orcidhttp://orcid.org/0000-0002-8859-141X; Email: loido@uh.edu

Authors

Babak Tahmouresilerd - Department of Chemistry, University of Houston, 4800 Calhoun Rd., Houston, Texas 77204, United States; https://orcid.org/0000-0002-7395-4572; Email: btahmour@uh.edu

Dawei Xiao - Department of Chemistry, University of Houston, 4800 Calhoun Rd., Houston, Texas 77204, United States

Author Contributions

The manuscript was written through contributions of all authors. All authors have given approval to the final version of the manuscript.

Notes

The authors declare no competing financial interest.

ACKNOWLEDGMENT

We are grateful to the Welch Foundation (E-1894) and the National Science Foundation (CHE-1750411) for grant support. We thank Prof. Tom Teets for allowing us to use a potentiostat for electrochemical measurements.

REFERENCES

(1) Chung, T. C. M. *Functionalization of Polyolefins*; Academic Press: San Diego, CA, 2002.
(2) Chen, E. Y.-X. Coordination Polymerization of Polar Vinyl Monomers by Single-Site Metal Catalysts. *Chem. Rev.* **2009**, *109*, 5157-5214.
(3) Guan, Z.; Cotts, P. M.; McCord, E. F.; McLain, S. J. Chain Walking: A New Strategy to Control Polymer Topology. *Science* **1999**, *283*, 2059-2062.
(4) Boffa, L. S.; Novak, B. M. Copolymerization of Polar Monomers With Olefins Using Transition-Metal Complexes. *Chem. Rev.* **2000**, *100*, 1479-1493.
(5) Ittel, S. D.; Johnson, L. K.; Brookhart, M. Late-Metal Catalysts for Ethylene Homo- and Copolymerization. *Chem. Rev.* **2000**, *100*, 1169-1203.
(6) Coates, G. W. Polymerization Catalysis at the Millennium: Frontiers in Stereoselective, Metal-Catalyzed Polymerization. *J. Chem. Soc., Dalton Trans.* **2002**, 467-475.
(7) Sita, L. R. Ex Uno Plures ("Out of One, Many"): New Paradigms for Expanding the Range of Polyolefins through Reversible Group Transfers. *Angew. Chem., Int. Ed.* **2009**, *48*, 2464-2472.
(8) Mu, H.; Zhou, G.; Hu, X.; Jian, Z. Recent Advances in Nickel Mediated Copolymerization of Olefin with Polar Monomers. *Coord. Chem. Rev.* **2021**, *435*, 213802.
(9) Walsh, D. J.; Hyatt, M. G.; Miller, S. A.; Guironnet, D. Recent Trends in Catalytic Polymerizations. *ACS Catal.* **2019**, 11153-11188.
(10) Chen, C. Designing Catalysts for Olefin Polymerization and Copolymerization: Beyond Electronic and Steric Tuning. *Nat. Rev. Chem.* **2018**, *2*, 6-14.
(11) Tan, C.; Chen, C. Emerging Palladium and Nickel Catalysts for Copolymerization of Olefins with Polar Monomers. *Angew. Chem., Int. Ed.* **2019**, *58*, 7192-7200.
(12) Kuhn, P.; Sémeril, D.; Matt, D.; Chetcuti, M. J.; Lutz, P. Structure-Reactivity Relationships in SHOP-type Complexes: Tunable Catalysts for the Oligomerisation and Polymerisation of Ethylene. *Dalton Trans.* **2007**, 515-528.
(13) Keim, W. Oligomerization of Ethylene to α-Olefins: Discovery and Development of the Shell Higher Olefin Process (SHOP). *Angew. Chem., Int. Ed.* **2013**, *52*, 12492-12496.
(14) Drent, E.; van Dijk, R.; van Ginkel, R.; van Oort, B.; Pugh, R. I. Palladium Catalysed Copolymerisation of Ethene with Alkylacrylates: Polar Comonomer Built into the Linear Polymer Chain. *Chem. Commun.* **2002**, 744-745.
(15) Carrow, B. P.; Nozaki, K. Synthesis of Functional Polyolefins Using Cationic Bisphosphine Monoxide‑Palladium Complexes. *J. Am. Chem. Soc.* **2012**, *134*, 8802-8805.
(16) Mitsushige, Y.; Yasuda, H.; Carrow, B. P.; Ito, S.; Kobayashi, M.; Tayano, T.; Watanabe, Y.; Okuno, Y.; Hayashi, S.; Kuroda, J.; Okumura, Y.; Nozaki, K. Methylene-Bridged Bisphosphine Monoxide Ligands for Palladium-Catalyzed Copolymerization of Ethylene and Polar Monomers. *ACS Macro Lett.* **2018**, *7*, 305-311.
(17) Nakamura, A.; Anselment, T. M. J.; Claverie, J.; Goodall, B.; Jordan, R. F.; Mecking, S.; Rieger, B.; Sen, A.; van Leeuwen, P. W. N. M.; Nozaki, K. *Ortho*-Phosphinobenzenesulfonate: A Superb Ligand for Palladium-Catalyzed Coordination-Insertion Copolymerization of Polar Vinyl Monomers. *Acc. Chem. Res.* **2013**, *46*, 1438-1449.
(18) Johnson, L.; Wang, L.; McLain, S.; Bennett, A.; Dobbs, K.; Hauptman, E.; Ionkin, A.; Ittel, S.; Kunitsky, K.; Marshall, W.; McCord, E.; Radzewich, C.; Rinehart, A.; Sweetman, K. J.; Wang, Y.; Yin, Z.; Brookhart, M. Copolymerization of Ethylene and Acrylates by Nickel Catalysts. In *Beyond Metallocenes*; American Chemical Society: 2003; Vol. 857, p 131-142.
(19) Komon, Z. J. A.; Bu, X.; Bazan, G. C. Synthesis of Butene−Ethylene and Hexene−Butene−Ethylene Copolymers from Ethylene via Tandem Action of Well-Defined Homogeneous Catalysts. *J. Am. Chem. Soc.* **2000**, *122*, 1830-1831.
(20) Cai, Z.; Xiao, D.; Do, L. H. Fine-Tuning Nickel Phenoxyimine Olefin Polymerization Catalysts: Performance Boosting by Alkali Cations. *J. Am. Chem. Soc.* **2015**, *137*, 15501-15510.
(21) Cai, Z.; Do, L. H. Customizing Polyolefin Morphology by Selective Pairing of Alkali Ions with Nickel Phenoxyimine-Polyethylene Glycol Catalysts. *Organometallics* **2017**, *36*, 4691-4698.
(22) Contrella, N. D.; Sampson, J. R.; Jordan, R. F. Copolymerization of Ethylene and Methyl Acrylate by Cationic Palladium Catalysts That Contain Phosphine-Diethyl Phosphonate Ancillary Ligands. *Organometallics* **2014**, *33*, 3546-3555.

(23) Cai, Z.; Do, L. H. Thermally Robust Heterobimetallic Palladium‐Alkali Catalysts for Ethylene and Alkyl Acrylate Copolymerization. *Organometallics* **2018**, *37*, 3874-3882.
(24) Xiao, D.; Cai, Z.; Do, L. H. Accelerating Ethylene Polymerization Using Secondary Metal Ions in Tetrahydrofuran. *Dalton Trans.* **2019**, *48*, 17887-17897.
(25) McCarthy, B. D.; Donley, C. L.; Dempsey, J. L. Electrode initiated proton-coupled electron transfer to promote degradation of a nickel(ii) coordination complex. *Chem. Sci.* **2015**, *6*, 2827-2834.
(26) Klug, C. M.; Dougherty, W. G.; Kassel, W. S.; Wiedner, E. S. Electrocatalytic Hydrogen Production by a Nickel Complex Containing a Tetradentate Phosphine Ligand. *Organometallics* **2019**, *38*, 1269-1279.
(27) Bowmaker, G. A.; Boyd, P. D. W.; Campbell, G. K. Spectroelectrochemistry of Nickel Complexes. Voltammetric and ESR Studies of the Redox Reactions of Phosphine-Dithiolate and Phosphine-Catecholate Complexes of Nickel. *Inorg. Chem.* **1982**, *21*, 2403-2412.
(28) Renny, J. S.; Tomasevich, L. L.; Tallmadge, E. H.; Collum, D. B. Method of Continuous Variations: Applications of Job Plots to the Study of Molecular Associations in Organometallic Chemistry. *Angew. Chem., Int. Ed.* **2013**, *52*, 11998-12013.
(29) Thordarson, P. Determining Association Constants from Titration Experiments in Supramolecular Chemistry. *Chem. Soc. Rev.* **2011**, *40*, 1305-1323.
(30) Brynn Hibbert, D.; Thordarson, P. The Death of the Job Plot, Transparency, Open Science and Online Tools, Uncertainty Estimation Methods and Other Developments in Supramolecular Chemistry Data Analysis. *Chem. Commun.* **2016**, *52*, 12792-12805.
(31) http://supramolecular.org (accessed July 2021)
(32) Jung, J.; Yasuda, H.; Nozaki, K. Copolymerization of Nonpolar Olefins and Allyl Acetate Using Nickel Catalysts Bearing a Methylene-Bridged Bisphosphine Monoxide Ligand. *Macromolecules* **2020**, *53*, 2547-2556.
(33) Hong, C.; Sui, X.; Li, Z.; Pang, W.; Chen, M. Phosphine Phosphonic Amide Nickel Catalyzed Ethylene Polymerization and Copolymerization with Polar Monomers. *Dalton Trans.* **2018**, *47*, 8264-8267.
(34) Ito, S. Effect of the backbone structure of bidentate ligands in palladium- and nickel-catalyzed polar monomer copolymerization. *Science China Chemistry* **2018**, *61*, 1349-1350.
(35) Zou, C.; Pang, W.; Chen, C. Influence of chelate ring size on the properties of phosphine-sulfonate palladium catalysts. *Science China Chemistry* **2018**, *61*, 1175-1178.
(36) Calculations were perfomred as follows: v_{growth} = yield of polymer/[moles of catalyst × MW of monomer × time]; $v_{transfer}$ = yield of polymer/[moles of catalyst × MW of polymer × time].
(37) Akita, S.; Nozaki, K. Copolymerization of Ethylene and Methyl Acrylate by Palladium Catalysts Bearing IzQO Ligands Containing Methoxyethyl Ether Moieties and Salt Effects for Polymerization. *Polym. J.* **2021**, *53*, 1057‐1060.
(38) Tran, T. V.; Karas, L. J.; Wu, J. I.; Do, L. H. Elucidating Secondary Metal Cation Effects on Nickel Olefin Polymerization Catalysts. *ACS Catal.* **2020**, *10*, 10760-10772.
(39) Puskas, J. E.; Kaszas, G. Carbocationic Polymerization. *Enc. Polym. Sci. Tech.* **2016**, 1-43.
(40) Cui, L.; Jian, Z. A *N*-Bridged Strategy Enables Hemilabile Phosphine‐Carbonyl Palladium and Nickel Catalysts to Mediate Ethylene Polymerization and Copolymerization with Polar Vinyl Monomers. *Polym. Chem.* **2020**, *11*, 6187-6193.
(41) Zhang, Y.; Mu, H.; Pan, L.; Wang, X.; Li, Y. Robust Bulky [P,O] Neutral Nickel Catalysts for Copolymerization of Ethylene with Polar Vinyl Monomers. *ACS Catal.* **2018**, *8*, 5963-5976.
(42) Wang, X.-l.; Zhang, Y.-p.; Wang, F.; Pan, L.; Wang, B.; Li, Y.-s. Robust and Reactive Neutral Nickel Catalysts for Ethylene Polymerization and Copolymerization with a Challenging 1,1-Disubstituted Difunctional Polar Monomer. *ACS Catal.* **2021**, *11*, 2902-2911.
(43) Xin, B. S.; Sato, N.; Tanna, A.; Oishi, Y.; Konishi, Y.; Shimizu, F. Nickel Catalyzed Copolymerization of Ethylene and Alkyl Acrylates. *J. Am. Chem. Soc.* **2017**, *139*, 3611-3614.
(44) Saki, Z.; D'Auria, I.; Dall'Anese, A.; Milani, B.; Pellecchia, C. Copolymerization of Ethylene and Methyl Acrylate by Pyridylimino Ni(II) Catalysts Affording Hyperbranched Poly(ethylene-co-methyl acrylate)s with Tunable Structures of the Ester Groups. *Macromolecules* **2020**, *53*, 9294-9305.
(45) Liang, T.; Goudari, S. B.; Chen, C. A Simple and Versatile Nickel Platform for the Generation of Branched High Molecular Weight Polyolefins. *Nat. Commun.* **2020**, *11*, 372.
(46) Zou, C.; Liao, D.; Pang, W.; Chen, M.; Tan, C. Versatile PNPO Ligands for Palladium and Nickel Catalyzed Ethylene Polymerization and Copolymerization with Polar Monomers. *J. Catal.* **2021**, *393*, 281-289.
(47) Chen, M.; Chen, C. A Versatile Ligand Platform for Palladium- and Nickel-Catalyzed Ethylene Copolymerization with Polar Monomers. *Angew. Chem., Int. Ed.* **2018**, *57*, 3094-3098.
(48) Xu, M.; Yu, F.; Li, P.; Xu, G.; Zhang, S.; Wang, F. Enhancing Chain Initiation Efficiency in the Cationic Allyl-Nickel Catalyzed (Co)Polymerization of Ethylene and Methyl Acrylate. *Inorg. Chem.* **2020**, *59*, 4475-4482.
(49) Li, M.; Wang, X.; Luo, Y.; Chen, C. A Second-Coordination-Sphere Strategy to Modulate Nickel- and Palladium-Catalyzed Olefin Polymerization and Copolymerization. *Angew. Chem., Int. Ed.* **2017**, *56*, 11604-11609.
(50) Piers, W. E.; Collins, S. Mechanistic Aspects of Olefin-Polymerization Catalysis. *Comp. Organomet. Chem. III* **2007**, *1*, 141-165.
(51) Xiong, S. Y.; Shoshani, M. M.; Zhang, X. L.; Spinney, H. A.; Nett, A. J.; Henderson, B. S.; Miller, T. F.; Agapie, T. Efficient Copolymerization of Acrylate and Ethylene with Neutral P, O-Chelated Nickel Catalysts: Mechanistic Investigations of Monomer Insertion and Chelate Formation. *J. Am. Chem. Soc.* **2021**, *143*, 6516-6527.

Table of Contents Graphic

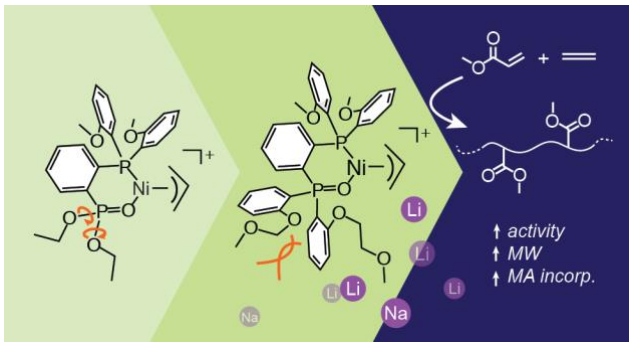

Synopsis

An iterative design approach was used to construct conformationally rigid nickel catalysts for ethylene and methyl acrylate copolymerization. These complexes exhibited greater catalytic activity and gave copolymers with higher molecular weight and polar monomer incorporation than earlier generations. The addition of alkali ions was also shown to have beneficial effects on polymerization.